Mon. Not. R. Astron. Soc. **000**, 1–11 (2019) Printed 8 November 2019 (MN LATEX style file v2.2)

Fundamental properties of stars from *Kepler* and *Gaia* data – parallax offset and revised scaling relations

M. Yıldız⋆ and S. Örtel

Department of Astronomy and Space Sciences, Science Faculty, Ege University, 35100, Bornova, İzmir, Turkey

Accepted 2019 May 15. Received 2019 April 11; in original form 2019 April 11

ABSTRACT

Thanks to the space missions *Gaia*, *Kepler*, *CoRoT* and *TESS*, we can obtain and confront distance from the parallax with asteroseismic distance ($d_{\rm DR2}$). We show that there is a relationship between radius from asteroseismic scaling relation ($R_{\rm sis}$) and non-asteroseismic measurements ($R_{\rm DR2}$) for main-sequence (MS) and sub-giant (SG) stars: $R_{\rm DR2}/{\rm R}_{\odot} = (1.052 \pm 0.010)(R_{\rm sis}/{\rm R}_{\odot})^{0.935\pm0.006}$. We extend our studies to the red-giant (RG) stars in APOKASC2 catalog and RGs in eclipsing binaries. We confirm very similar relations between $R_{\rm DR2}$ and $R_{\rm sis}$ for RGs. The modified $R_{\rm sis}$ makes $d_{\rm sis}$ in very good agreement with $d_{\rm DR2}$. From the ratio $\sqrt{(R_{\rm DR2}/R_{\rm sis})^3/(M_{\rm DR2}/M_{\rm sis})}$ we obtain an expression for the corrected relation ($f_{\Delta\nu}$) between the mean large separation and mean density. This expression for MS and SG stars is very close to the one obtained from interior MS models by Yıldız et al. (2016). For the coolest RGs, we derive a new expression for $f_{\Delta\nu}$. According to our findings, mass and radius of 1323 RGs range about 0.9-1.5 ${\rm M}_{\odot}$ and 4.2-48 ${\rm R}_{\odot}$, respectively. Other very important effects for the source of the difference between asteroseismic and non-asteroseismic stellar parameters may be due to uncertainty in effective temperature ($T_{\rm eff}$) and parallax offset. We can modify $T_{\rm eff}$ in order to make $R_{\rm sis}$ and $R_{\rm DR2}$ equal, because the dependencies of $R_{\rm sis}$ and $R_{\rm DR2}$ on $T_{\rm eff}$ are completely different. For 1160 stars of 1323 RGs, the difference between $T_{\rm eff}$ from APOKASC2 and modified $T_{\rm eff}$ is less than 200 K. We find relation between scaling parameters and parallax offset and also show that the offsets derived for RG stars and stars around MS and SG phases are very different.

Key words: stars: distance – stars: evolution – stars: fundamental parameters – stars: interiors – stars: late-type – stars: oscillations.

1 INTRODUCTION

Determination of stellar properties is very important for our understanding of astronomical structures from planets to galaxies. Thanks to the *Kepler* (Borucki et al. 2010), *CoRoT* (Baglin et al. 2006) and *TESS* (Sullivan et al. 2015) space telescopes, asteroseismic scaling relations are very useful to estimate fundamental stellar parameters. One of the essential data that we require in discovering fundamental stellar properties or to check the relations between these properties is the distance of stars to us. We have already compared asteroseismic distances ($d_{\rm sis}$) derived from the so-called asteroseismic scaling relations with the *Gaia* (Gaia Collaboration et al. 2016) distances ($d_{\rm DR1}$) from DR1 (Yıldız et al. 2017). There was a good agreement between them for the 64 stars, the difference was less than 10 per cent. In the present study, we compare $d_{\rm sis}$ and the recent *Gaia* distances ($d_{\rm DR2}$; DR2, Gaia Collaboration et al. 2018) and try to improve asteroseismic relations, using data of solar-like oscillating stars in eclipsing binaries (EB; Gaulme et al. 2016) and red-giants (RGs) in APOKASC2 (Pinsonneault et al. 2018). The total number of analyzed stars is about 1800. We also discuss parallax zero-point offset with and without improved scaling relations.

For computation of asteroseismic distance of a star, the most important outcome of asteroseismology is the scaling relation for radius ($R_{\rm sis}$), which relate radius to so-called large separation between oscillation frequencies ($\langle\Delta\nu\rangle$), frequency of maximum amplitude ($\nu_{\rm max}$) and effective temperature ($T_{\rm eff}$). Then using R and spectroscopic $T_{\rm eff}$, one can obtain luminosity and hence distance of the star. If we have highly precise parallaxes, the comparison of $d_{\rm sis}$ and $d_{\rm DR2}$ will enlighten how the asteroseismic relation for R is admissible and how spectroscopic measurement of $T_{\rm eff}$ is successful. For computation of stellar mass from $d_{\rm DR2}$, the surface gravity of stars ($\log g$) should also be very precisely determined.

It is well known that sound speed is a function of compress-

⋆ E-mail: mutlu.yildiz@ege.edu.tr

ibility (Γ_1), in addition to temperature. In deriving scaling relations between asteroseismic and non-asteroseismic quantities, compressibility at the stellar surfaces (Γ_{1s}) is taken as a constant. However, Yıldız et al. (2016) have shown that Γ_{1s} is not constant at the stellar surfaces and modified the expressions for $\nu_{\max}$ and $\Delta\nu$ as functions of Γ_{1s}. They also obtain how compressibility depends on $T_{\rm eff}$ for main-sequence (MS) stars. A similar modification of scaling relation should be done over mean molecular weight for hot stars and in particular for red-giants, in which molecular formation might be significant in the surface regions.

De Ridder et al. (2016) found excellent agreement between $d_{\rm sis}$ and $d_{\rm DR1}$ for 22 dwarfs and sub-giant solar-like oscillators. They also confirm that $d_{\rm DR1}$ is more uncertain than $d_{\rm sis}$ for a sample of 938 red giant solar-like oscillators ($d_{\rm sis} > 300$ pc), more distant than the pulsating dwarfs ($d_{\rm sis} < 250$ pc). Davies et al. (2017) compare the *Gaia* DR1 distances with $d_{\rm sis}$ of red clump stars and the distances obtained using luminosities determined by eclipsing binaries. They find that $d_{\rm sis}$ is in better agreement with the RC distance estimators than the DR1 distances. They propose a correction to $d_{\rm DR1}$ as a function of distances > 500 pc for the *Kepler* field-of-view. Huber et al. (2017) compare of parallaxes and radii from asteroseismology and *Gaia* DR1 for 2200 *Kepler* stars spanning from the main sequence to the red giant branch. They find no significant offset for main-sequence and low-luminosity RGs.

Stassun and Torres (2018) found empirical distances of eclipsing binaries and compared the distances from the *Gaia* DR2 parallaxes. They found that a systematic offset of -82 $\pm$ 33 μas, in the sense that the Gaia parallaxes being too small. A similar offset (52.8 $\pm$ 2.4 μas) is identified by Zinn et al. (2018) for the RGs from the APOKASC2 catalogue. Kallinger et al. (2018) and Sahlholdt et al. (2018) try to revise conventional asteroseismic scaling relations in order to obtain consistency between $d_{\rm sis}$ and $d_{\rm DR2}$. We show how parallax zero-point offset and improvements in scaling relations are interrelated (see section 5)

This paper is organized as follows: Section 2 presents DR2 distances and other observational data for about 1800 stars, and compares DR1 and DR2 distances of 74 stars. In section 3, we briefly explain the method for the computation of asteroseismic distance. Section 4 is devoted to the results and their comparison. Parallax offset issue is considered in section 5. Finally, in Section 6, our conclusions are drawn.

2 *Gaia* DISTANCES - COMPARISON OF DR1 AND DR2 DATA

We have studied 89 solar-like oscillating stars in Yıldız et al. (2016, 2019). Parallaxes of 74 of these stars are available in DR1. Their $d_{\rm sis}$ and $d_{\rm DR1}$ are already compared in Yıldız et al. (2017). Their distances range 21-433 pc.

$d_{\rm DR2}$ of 74 solar-like oscillating stars is plotted with respect to $d_{\rm DR1}$ in Fig.1, with their uncertainties. The difference between $d_{\rm DR2}$ and $d_{\rm DR1}$ is less than 4 per cent for 54 stars and greater than 10 per cent for 7 stars. The systematic difference is about 2.4 per cent. The greatest differences occur for KIC 8379927/HIP 97321 and KIC 1435467. The difference between their $d_{\rm DR1}$ and $d_{\rm DR2}$ are 27 and 30 per cent, respectively. For five stars, namely, KIC 4914923/HIP 94734, KIC 6933899, KIC 12317678/HIP 97316, KIC 12508433 and HD 181907/HIP 95222, the difference between the distances is about 9-13 per cent.

We notice that $d_{\rm DR2}$ is much more precise than $d_{\rm DR1}$. In Fig. 2, uncertainty in $d_{\rm DR2}$ ($\Delta d_{\rm DR2}$) is plotted with respect to uncertainty in $d_{\rm DR1}$ ($\Delta d_{\rm DR1}$) . The solid line is the fitted line of $11.7x$. The implication is that $\Delta d_{\rm DR2}$ is about one twelfth of $\Delta d_{\rm DR1}$.

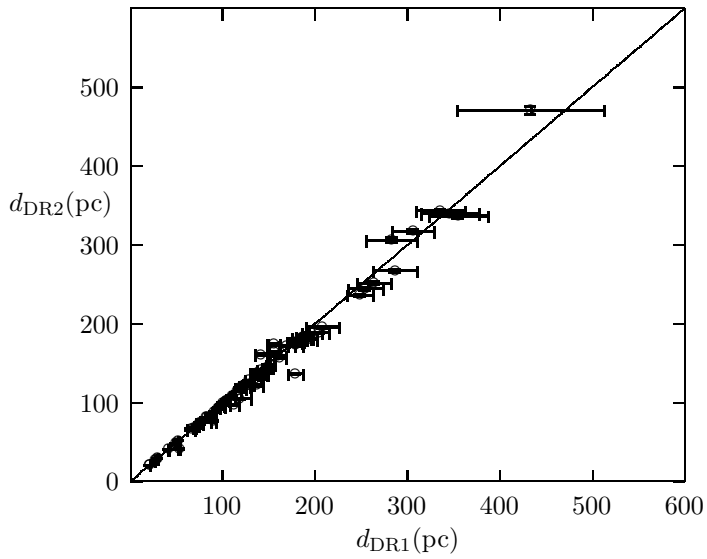

Figure 1. $d_{\rm DR2}$ of 74 stars is plotted with respect to $d_{\rm DR1}$ in units of pc.

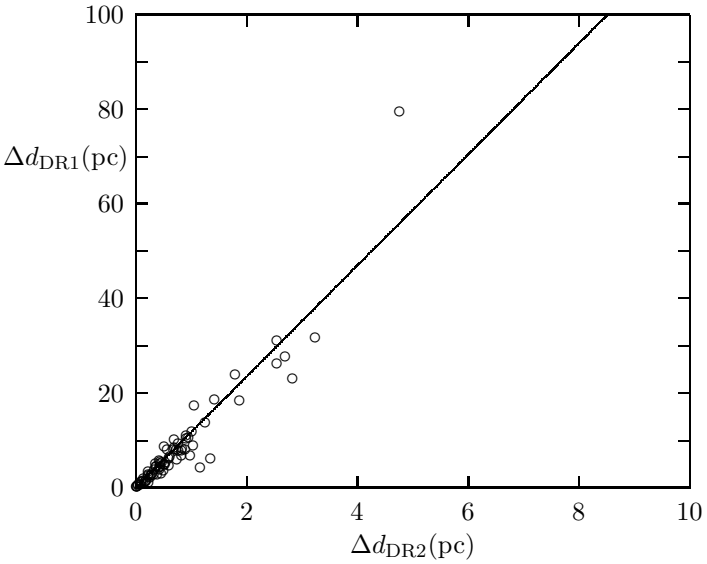

Figure 2. $\Delta d_{\rm DR1}$ of 74 stars is plotted with respect to $\Delta d_{\rm DR2}$ in units of pc. The solid line is the fitted line of $11.7x$. This implies that $d_{\rm DR2}$ is about 12 times more precise than $d_{\rm DR1}$.

In addition to the 74 stars, parallaxes of five more solar-like oscillating stars studied in Yıldız et al. (2016) are available in DR2. These stars are KIC 8219268, KIC 11026764, HD 43587/HIP 29860, HD 146233/HIP 79672 and HD 203608/HIP 105858. The latter three stars are relatively very close to the Sun, the closest stars among the 79 stars. Their distances are 19.30, 14.13 and 9.27 pc, respectively. Their solar-like oscillations were detected from *CoRoT* light curve. KIC 8219268 and KIC 11026764 were among the *Kepler* targets. The $d_{\rm DR2}$ of KIC 11026764 is 156.89 pc, while KIC 8219268 is 1345 pc apart and the farthest of the 79 stars. It is a red giant and its radius is about 6.7 $R_\odot$.

The analysis of 79 stars leads us to extend this study to include red giants. In addition to the solar-like oscillating red giants

in eclipsing binaries, we also consider 909 RGs from APOKASC2 for which the *Gaia* DR2 parallax and V are available. Their distance range 200-11250 pc. While most of the 909 RGs have a $d_{\rm DR2}$ less than 4000 pc, there are only 10 giants with $d_{\rm DR2} > 6000$ pc. V of these RGs are taken from the SIMBAD database, compiled from different sources. For more uniform data, we also use G of the RGs from the *Gaia* database. The number of stars for which the interstellar extinction A_g is available and are also shown in APOKASC2 is 1323. For these stars, effective temperature ($T_{\rm G}$) and R are also available in the *Gaia* database. This is a very good occasion to compare our computations with *Gaia* results for radius. We can also assess which of *Gaia* and APOKASC2 $T_{\rm eff}$s ($T_{\rm A}$) are more convenient for the agreement between $d_{\rm sis}$ and $d_{\rm DR2}$.

Using the distance of stars and V, we can compute absolute magnitude and then their luminosity. For the computation of luminosity, BC is derived by interpolating between the colour-$T_{\rm eff}$ tables of Lejeune, Cuisinier & Buser (1998) or MIST (Choi et al. 2016). Since we have the $T_{\rm eff}$ of stars from their spectroscopic observations ($T_{\rm eS}$), the radius of stars ($R_{\rm DR2}$) can be obtained from $L = 4\pi R^2_{\rm DR2} T^4_{\rm eff}$. Using either spectroscopic ($\log g_{\rm S}$) or asteroseismic ($\log g_{\rm sis}$) gravity, stellar mass can also be utilized. For a reliable stellar mass, in addition to distance with a small uncertainty, a very precise $\log g$ value is required.

3 ASTEROSEISMIC DISTANCES, MASSES AND RADII

$d_{\rm sis}$ and distance uncertainty ($\Delta d_{\rm sis}$) of the solar-like oscillating stars are computed as in Yıldız et al. (2017). In short, in order to compute distance modulus from absolute magnitude, we must first obtain luminosity. The luminosity of these stars is computed using $T_{\rm eff}$ and $R_{\rm sis}$. In addition to these quantities, visual magnitude V (or G), metallicity ($[Fe/H]$) and bolometric correction BC are required for computation of $d_{\rm sis}$ of a star. We use both the conventional and modified (equations 9 and 10 in Yıldız et al. 2016, respectively) asteroseismic scaling relations to obtain the mass and radius of the stars.

The scaling relations for M and R are based on two expressions for $\Delta\nu$ and $\nu_{\rm max}$.

$$\frac{\langle\Delta\nu\rangle}{\langle\Delta\nu_\odot\rangle} = f_{\Delta\nu}\frac{\langle\rho\rangle}{\langle\rho_\odot\rangle^{1/2}} \quad (1)$$

where $f_{\Delta\nu}$ may either represent physical condition difference between the stellar and solar surfaces which are effective on $\langle\Delta\nu\rangle$ or evaluates how valid is our assumptions behind the procedure in derivation of the scaling relations. Similarly,

$$\frac{\nu_{\rm max}}{\nu_{\rm max\odot}} = f_{\nu_{\rm max}}\frac{g/g_\odot}{(T_{\rm eff}/T_{\rm eff\odot})^{1/2}}. \quad (2)$$

$f_{\nu_{\rm max}}$ may have the same physical meaning as $f_{\Delta\nu}$. The conventional scaling relations assume $f_{\nu_{\rm max}}$ and $f_{\Delta\nu}$ unity. For the solar-like oscillating MS stars, this can be a good approach. The structure of evolved stars is however significantly different from the solar structure. In this case, $R_{\rm sis}$, which is used in computation of $d_{\rm sis}$ and proportional to $\nu_{\rm max}/\langle\Delta\nu\rangle^2$, must be multiplied by $f^2_{\Delta\nu}/f_{\nu_{\rm max}}$. For $M_{\rm sis}$, the factor is $f^4_{\Delta\nu}/f^3_{\nu_{\rm max}}$. Most of the stars in the APOKASC2 catalog are evolved RG stars. Their high brightness allows detection of their solar-like oscillations by the *Kepler* and *CoRoT* telescopes, despite their wide spread in Galactic Disk. Therefore, any improvement in scaling relations for these stars will be a substantial advancement not only in stellar astrophysics but also in our understanding of chemical evolution and dynamics of Galactic Disk. $f_{\nu_{\rm max}}$ is related to f_ν introduced by Yıldız et al. (2016) as

$$f_{\nu_{\rm max}} = f_\nu\left(\frac{\mu_{\rm s}\Gamma_{1\rm s}}{\mu_{\rm s\odot}\Gamma_{1\rm s\odot}}\right)^{1/2} \quad (3)$$

where $\mu_{\rm s}$ is the mean molecular weight at the stellar surface.

The solar values of $\langle\Delta\nu_\odot\rangle$ and $\nu_{\rm max\odot}$ are taken as 136 and 3050 μHz, respectively.

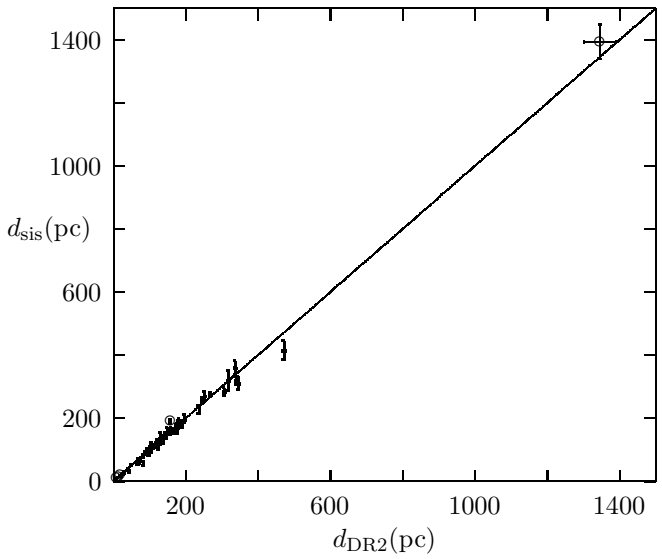

Figure 3. $d_{\rm sis}$ of 79 stars is plotted with respect to $d_{\rm DR2}$ in units of pc. 5 stars for which DR1 data is not available are represented by circle.

4 RESULTS AND DISCUSSIONS

4.1 Comparison of distances of 79 stars

$d_{\rm sis}$ is plotted with respect to $d_{\rm DR2}$ in Fig. 3 for 74 stars studied in Yıldız al. (2017) and 5 stars for which only $d_{\rm DR2}$ is available. There is in general a very good agreement between $d_{\rm sis}$ and $d_{\rm DR2}$ of 79 stars. The most striking feature of Fig. 1 is to see how successful both asteroseismic and astrometric methods in determination of distance of a star at 1345 pc (KIC 8219268). The seven stars for which the great differences occur between $d_{\rm DR2}$ and $d_{\rm DR1}$ (section 2) are listed in Table 1. For five of them, their $d_{\rm DR2}$ are in better agreement with their $d_{\rm sis}$ than $d_{\rm DR1}$, in particular for KIC 1435467, KIC 4914923 and KIC 6933899. For two of the seven stars, however, $d_{\rm DR1}$ is in better agreement with $d_{\rm sis}$ rather than $d_{\rm DR2}$. For HD 181907, $d_{\rm sis}$ and $d_{\rm DR1}$ are very close to each other.

The fractional difference between $d_{\rm DR2}$ and $d_{\rm sis}$ is plotted with respect to $\log d_{\rm DR2}$ in Fig. 4. The systematic difference between these distances is about 1.6 per cent for 74 stars and 1.1 per cent for 79 stars. In Yıldız et al. (2017), the difference between $d_{\rm DR1}$ and $d_{\rm sis}$ was about 5 per cent. This shows that $d_{\rm DR2}$ is more precise than $d_{\rm DR1}$. If we compute BC from MIST tables rather than Lejeune et al. (1998), the systematic difference between $d_{\rm DR2}$ and $d_{\rm sis}$ for the 74 stars is just 0.3 per cent.

For 59 of the 79 stars, the difference between $d_{\rm DR2}$ and $d_{\rm sis}$ (δd) is less than 6 per cent. We notice that distance of most of the stars with $\delta d/d < 0.06$ is less than 200 pc. The largest fractional differences ($\delta d/d$) between $d_{\rm DR2}$ and $d_{\rm sis}$ are 0.30 and -0.22 for

Table 1. Asteroseismic distance and distances from DR1 and DR2 for the seven stars with very different $d_{\rm DR1}$ and $d_{\rm DR2}$. Distances in good agreement with $d_{\rm sis}$ are printed in bold style. For five of the seven stars, $d_{\rm DR2}$ is in better agreement with $d_{\rm sis}$ than $d_{\rm DR1}$.

Star	$d_{\rm DR1}$(pc)	$d_{\rm DR2}$(pc)	$d_{\rm sis}$(pc)
KIC 1435467	178.6	**137.2**	**133.7**
KIC 4914923	137.5	**122.4**	**122.7**
KIC 6933899	141.9	**161.7**	**160.1**
KIC 8379927	53.3	**41.9**	**34.6**
KIC 10454113	112.5	**97.6**	**86.9**
KIC 12508433	**155.2**	174.4	**161.1**
HD 181907	**118.5**	105.6	**119.6**

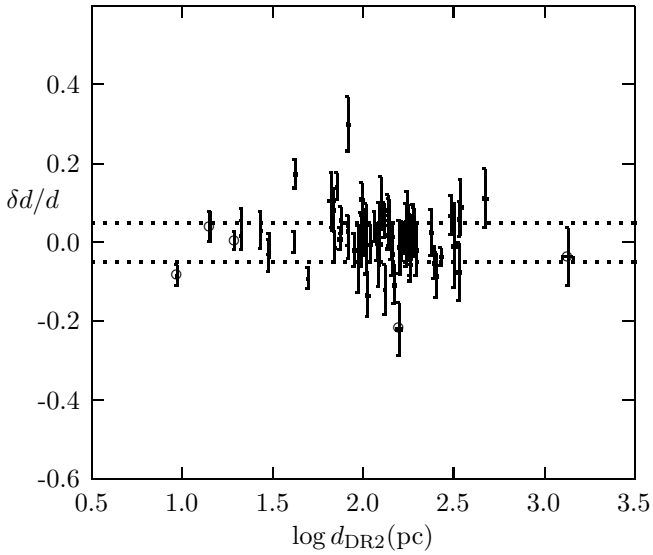

Figure 4. $\delta d/d$ of 79 stars is plotted with respect to $\log d_{\rm DR2}$. 5 stars for which DR1 data is not available are represented by circle.

KIC 9025370 and KIC 11026764, respectively. The difference between DR1 and DR2 distances of KIC 9025370 is about 6 per cent. KIC 9025370 has the most uncertain $\nu_{\rm max}$ ($\nu_{\rm max} = 215\mu$Hz) among the 79 stars. The difference between the distances may arise from this fact.

If we use the modified scaling relation for radius of stars with $\Gamma_{1\rm s}$ (equation 10 in Yıldız et al. 2016 with $f_{\nu_{\rm max}} = 1$), then the systematic difference between $d_{\rm sis}$ and $d_{\rm DR2}$ is about 1.8 per cent. Although there is a slight difference between distances computed from conventional and modified scaling relations, the situation changes if we compare $R_{\rm sis}$ and $R_{\rm DR2}$ (see below).

Spectroscopic gravity ($\log g_{\rm S}$) of stars is perhaps the most uncertain parameter derived from spectroscopic observations. We prepare another sample of stars for which difference between $\log g_{\rm S}$ and $\log g_{\rm sis}$ is less than 5 per cent. 32 stars are involved in this sample. For this sample, the systematic difference between $d_{\rm sis}$ and $d_{\rm DR2}$ is about 0.4 per cent, much smaller than that of 79 stars. If $|\log g_{\rm S} - \log g_{\rm sis}| < 0.07$, the distance difference of 42 stars reduces to 0.1 per cent. Except 7 stars, the distance difference for all of the stars is less than 6 per cent. The largest difference occurs for KIC 11026764: $d_{\rm DR2}$=156.9, $d_{\rm DR1}$=184.0, $d_{\rm sis}$=191.27 pc. If we take $\nu_{\rm max}$=860 μHz, $d_{\rm sis}$ becomes 183.8 pc and in very good agreement with $d_{\rm DR1}$.

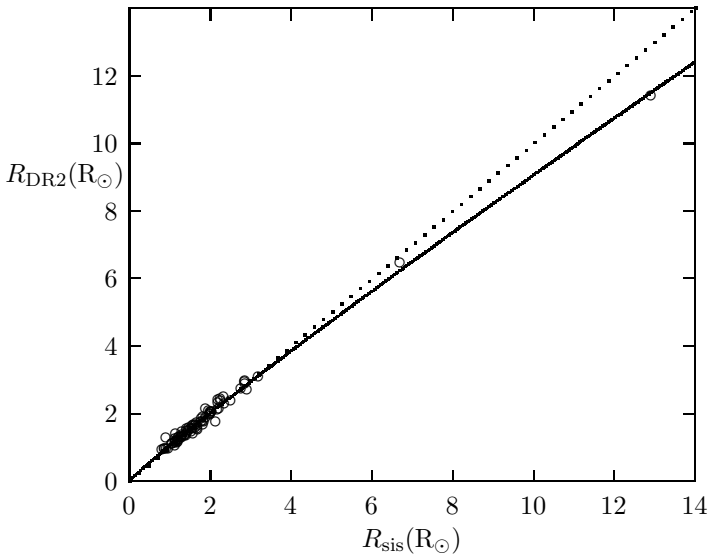

Figure 5. $R_{\rm DR2}$ of 79 stars is plotted with respect to $R_{\rm sis}$ in solar units. The solid line shows the fitting curve $(1.052 \pm 0.010)R_{\rm sis}^{0.935\pm0.006}$, and the dotted line is for $R_{\rm DR2} = R_{\rm sis}$.

4.2 Comparison of radii of the 79 stars

$R_{\rm DR2} = (L/4\pi T_{\rm eff}^4)^{1/2}$ of the 79 stars are plotted with respect to $R_{\rm sis}$ in Fig. 5. The radii of solar-like oscillating stars range 0.93-11.4 $\rm R_\odot$. The largest star is HD 181907. It is a RG and relatively close to us. Its distance is 105.6 pc. Its solar-like oscillations were detected by the *CoRoT* telescope. For small radii, $R_{\rm DR2}$ and $R_{\rm sis}$ are in good agreement. For the large values of radii, however, the data deviate from the $R_{\rm DR2} = R_{\rm sis}$ line. The fitting curve is found as $(1.052 \pm 0.010)(R_{\rm sis}/\rm R_\odot)^{0.935\pm0.006}$ (hereafter, radii and masses in similar relationships are written in solar units). There are apparent reasons for having doubts about if this deviation is real, since there are only 2 stars with radius larger than 3.5 $\rm R_\odot$. And, the $R_{\rm DR2} = R_{\rm sis}$ line and the curve apparently deviates after 3.5 $\rm R_\odot$. Therefore, we obtain another curve by subtracting the two largest stars. The new curve is found as $(1.040 \pm 0.017)R_{\rm sis}^{0.950\pm0.023}$. Two curves are very similar to each other. However, to be sure, data of the *Kepler* RG stars should be analyzed (see below).

Indeed, these curves have a problematic situation. For the Sun, for example, we will find its radius as 1.052 $\rm R_\odot$. In order to avoid such an undesirable situation we can change the adopted values of the solar $\langle\Delta\nu_\odot\rangle$ and $\nu_{\rm max\odot}$. Their values could be $\nu_{\rm max\odot}$ = 3000 μHz and $\langle\Delta\nu_\odot\rangle$= 138.5 μHz, for example. In that case, the first curve becomes $(1.001\pm0.010)R_{\rm sis}^{0.935\pm0.006}$. When these solar values are used, the systematic difference between $d_{\rm sis}$ and $d_{\rm DR2}$ increases (-4.2 per cent). When we take $\nu_{\rm max\odot}$= 2950 μHz and $\langle\Delta\nu_\odot\rangle$ = 136.0 μHz, the systematic difference is -2.2 per cent and the curve is $1.020R_{\rm sis}^{0.935}$.

In computation of $R_{\rm sis}$ and $R_{\rm DR2}$ we use the same $T_{\rm eff}$, therefore, $\delta d/d = (d_{\rm sis} - d_{\rm DR2})/d_{\rm sis}$ is equal to $\delta R/R = (R_{\rm sis} - R_{\rm DR2})/R_{\rm sis}$. The explanation is as following. For a given V of a star, we essentially know the ratio L/d^2. For precise determination of d, we must find L. For computation of L, we have spectroscopically or photometrically derived $T_{\rm eff}$ and $R_{\rm sis}$ obtained from asteroseismic scaling relations. Since we use the same $T_{\rm eff}$ in computation of $R_{\rm sis}$ and $R_{\rm DR2}$, the difference between $L_{\rm sis}$ and $L_{\rm DR2}$ is due to the difference between the radii $R_{\rm sis}$ and $R_{\rm DR2}$. In that

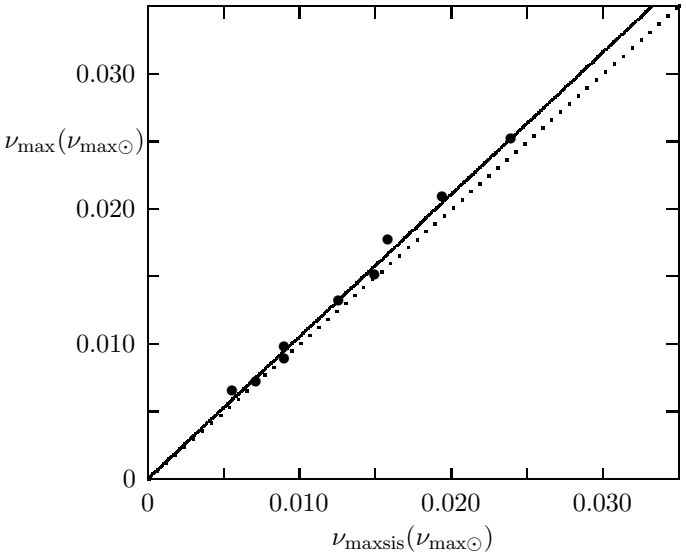

Figure 6. $\nu_{\rm max}$ of the 10 RGs in EBs is plotted with respect to $\nu_{\rm maxsis}$. The solid line is for the fitting line $1.052\nu_{\rm maxsis}$, while the dotted line represents $\nu_{\rm max} = \nu_{\rm maxsis}$.

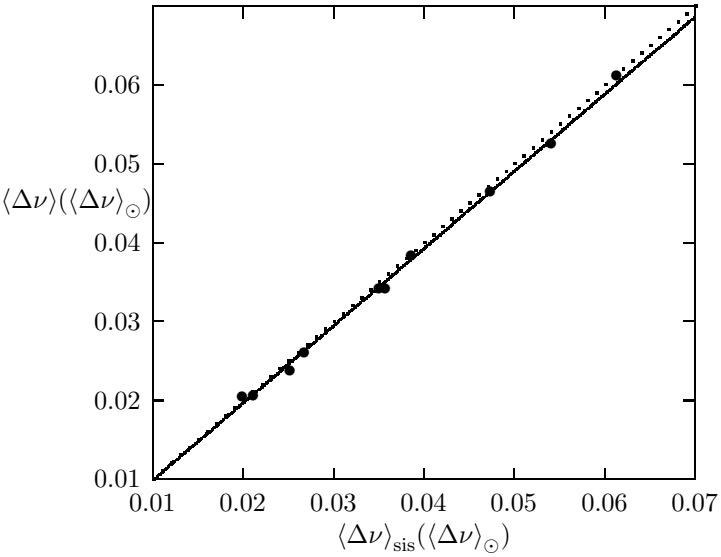

Figure 7. $\Delta\nu$ of the 10 RGs in EBs is plotted with respect to $\Delta\nu_{\rm sis}$. The solid line is for the fitting line $0.980\Delta\nu_{\rm sis}$, while the dotted line represents $\Delta\nu = \Delta\nu_{\rm sis}$.

case, $L/d^2 \propto R^2/d^2$. Since this ratio is constant for a given V, then $\delta d/d$ is equal to $\delta R/R$.

There is a substantial difference between $R_{\rm DR2}$ and $R_{\rm sis}$. We can correct the asteroseismic radius ($R_{\rm cor}$) according to the fitted curve from Fig. 5: $R_{\rm cor} = 1.052R_{\rm sis}^{0.935}$, where radii are in solar units (this is the case used for similar relationships between radii). If we use $R_{\rm cor}$ in place of $R_{\rm sis}$ and recalculate $d_{\rm sis}$, we see that $d_{\rm sis}$ and $d_{\rm DR2}$ are in better agreement. Their fractional difference is about -0.005 (-0.5 per cent; $d_{\rm sis}$ is 0.5 per cent greater than $d_{\rm DR2}$).

Although the correction in $R_{\rm sis}$ improves the agreement between $d_{\rm sis}$ and $d_{\rm DR2}$, $R_{\rm sis}$ deviates from $R_{\rm DR2}$ for only a few stars with large radius. This deviation can be tested using the red giant stars in the APOKASC2 catalog and solar-like oscillating RGs in eclipsing binaries.

4.3 Solar-like oscillating RGs in EBs and their implication for the scaling relations

For the 10 eclipsing binaries, mass ($M_{\rm rv}$) and radius ($R_{\rm rv}$) of the component stars are obtained by analyzing their light curves and radial velocities (Gaulme et al. 2016). The RG components in these binaries are solar-like oscillating stars. Their $\nu_{\rm max}$ and $\langle\Delta\nu\rangle$ are derived from the *Kepler* light curves. These stars are a good benchmark for testing the asteroseismic scaling relations. We can compare results of our computations in the previous sections with the asteroseismic and non-asteroseismic properties of solar-like oscillating RGs in EBs.

Gaulme et al. (2016) have already confirmed discrepancies between quantities (M and R) derived from asteroseismic and non-asteroseismic methods. We first compare the $\nu_{\rm max}$ and $\langle\Delta\nu\rangle$. In Fig. 6, the observed $\nu_{\rm max}$ is plotted with respect to $\nu_{\rm maxsis}$ where $\nu_{\rm maxsis}$ (in units of $\nu_{\rm max\odot} = 3050$ μHz) is computed using equation (2) assuming $f_{\nu_{\rm max}} = 1$, and g is computed from $M_{\rm rv}$ and $R_{\rm rv}$. There is a small but significant difference between $\nu_{\rm max}$ and $\nu_{\rm maxsis}$. The fitting line is $1.052\nu_{\rm maxsis}$. This fixes that $f_{\nu_{\rm max}} = 1.052$ for the RGs in 10 EBs.

In Fig. 7, $\langle\Delta\nu\rangle$ is plotted with respect to $\langle\Delta\nu_{\rm sis}\rangle$ in units of $\langle\Delta\nu_\odot\rangle$. They seem in good agreement. Nevertheless, the slope of the fitting line is 0.980. The difference, as much as 2 per cent, might be considered as very small, however influence of such a difference on R and M is 4 and 8 per cent, respectively. Therefore, we take into account this discrepancy in the scaling relations.

If we consider the 79 stars and the 10 RGs together for the relation between $R_{\rm DR2}$ and $R_{\rm sis}$, we obtain

$$R_{\rm DR2} = (1.039 \pm 0.013)R_{\rm sis}^{0.945\pm0.005}.$$

4.4 Comparison of distances and radii of RGs in APOKASC2

4.4.1 Comparison of distances of RGs using V

V and the DR2 parallax of 909 RGs from APOKASC2 are available from the SIMBAD database. We compute the asteroseismic and non-asteroseismic parameters of these stars using BC tables of MIST. The systematic difference between $d_{\rm DR2}$ and $d_{\rm sis}$ is about 12.5 per cent, much greater than the corresponding difference for the 79 stars. In Fig. 8, $R_{\rm DR2}$ of these stars is plotted with respect to $R_{\rm sis}$. The solid line shows the fitted curve: $R_{\rm DR2} = (1.070 \pm 0.032)R_{\rm sis}^{0.947\pm0.010}$. This relationship between the radii for this group of stars is very similar to that for 79 stars (see section 4.2 and Fig. 5). If we use the corrected radius (and maybe M) and recalculate $R_{\rm sis}$, the systematic difference reduces to 1.2 per cent.

The difference between $d_{\rm sis}$ and $d_{\rm DR2}$ is greater than 50 per cent for some stars. Such a big difference may be due to some unusual causes. For KIC 10273236, for example, the unusual difference between $d_{\rm sis}$ and $d_{\rm DR2}$, about 62 per cent, seems to arise from V. If we plot the V of stars with respect to K, there is a strict relationship between them. Some of the stars do not obey this relation. KIC 10273236 is among these stars and its V according to its K must be about 12.25 rather than 10.2. If we take V as 12.25, the difference reduces to 3 per cent. If we disregard such stars, we obtain relationship between $R_{\rm DR2}$ and $R_{\rm sis}$ as

$$R_{\rm DR2} = (1.029 \pm 0.024)R_{\rm sis}^{0.957\pm0.008}.$$

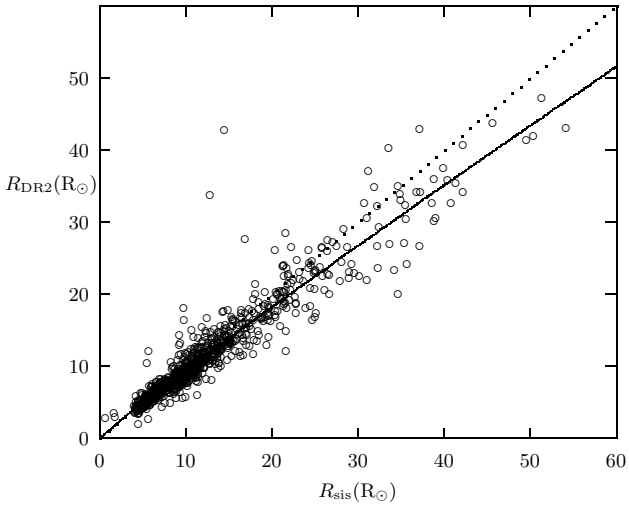

Figure 8. $R_{\rm DR2}$ of 909 stars is plotted with respect to $R_{\rm sis}$ in units of solar radius. The solid line shows the fitted curve $1.070R_{\rm sis}^{0.947}$, while the dotted line is for $R_{\rm DR2} = R_{\rm sis}$.

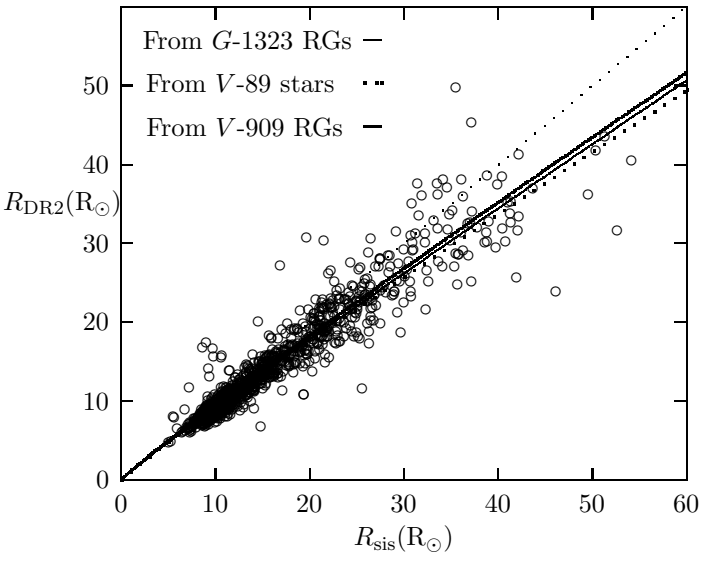

Figure 9. $R_{\rm DR2}$ of 1323 RG stars is plotted with respect to $R_{\rm sis}$ in solar units. $T_{\rm eff}$ is taken as $T_{\rm A}$. The thin solid line is the fitting curve: $(1.028 \pm 0.024)R_{\rm sis}^{0.952\pm0.008}$. Also shown are the fitting curves for the 89 (thick dotted line) and 909 RG stars (thick solid line). The thin dotted line is for $R_{\rm DR2} = R_{\rm sis}$.

4.4.2 Comparison of distances and radii of RGs using G magnitude

V magnitudes of stars in the SIMBAD database are compiled from different sources with different V band width. This may causes some problems because BC depends on the band width of measurements. Therefore, we also use *Gaia* catalog and use G magnitudes for the computation of BC. We find 1323 RGs from APOKASC2 for which G, A_g, $T_{\rm eff} = T_{\rm G}$ and R are available from the *Gaia* database. In Fig. 9, the $R_{\rm DR2}$ of these stars is plotted with respect to their $R_{\rm sis}$. For this figure, $T_{\rm eff}$ is taken from APOCASK2. The fitting curve is derived as

$$R_{\rm DR2} = (1.028 \pm 0.024)R_{\rm sis}^{0.952\pm0.008}.$$

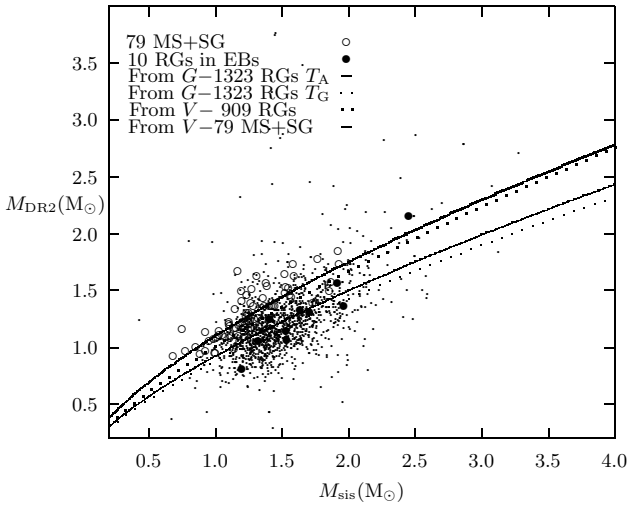

Figure 10. $M_{\rm DR2}$ of 1323 RG stars is plotted with respect to $M_{\rm sis}$ in solar units. $T_{\rm eff}$ is taken as $T_{\rm A}$. The thin solid and dotted lines are the fitting curves for 1323 stars with $T_{\rm A}$ $(0.925M_{\rm sis}^{0.698})$ and $T_{\rm G}$ $(0.884M_{\rm sis}^{0.698})$, respectively. Also shown are the fitting curves for the 79 (thick solid line) and 909 RG stars (thick dotted line).

We also obtain another fitting curve for radius using $T_{\rm eff} = T_{\rm G}$. This curve ($(0.956\pm0.023)R_{\rm sis}^{0.968\pm0.008}$) is almost the same as the curve for $T_{\rm eff} = T_{\rm A}$, despite apparent differences between factors and powers of $R_{\rm sis}$. Also shown are the fitting curves obtained for the 89 ($1.039R_{\rm sis}^{0.945}$ for 79 mainly MS and SG stars + 10 RGs in EBs) and 909 RGs ($1.070R_{\rm sis}^{0.947}$). These three curves are very similar to each other.

The $d_{\rm sis}$ and $d_{\rm DR2}$ of RG KIC 5395942/ Gaia DR2 2075037891998301312 are very different from each other. We therefore neglect this star in our analysis. The problem seems to be due to its parallax (13.09 mas).

4.5 Comparison of masses

The same gravity ($g_{\rm sis}$) and $T_{\rm eff}$ are used in computation of asteroseismic and non-asteroseismic distance, radius and mass. Therefore, δg is equal to zero. This implies that $\delta M/M = 2\delta R/R = 2(R_{\rm sis} - R_{\rm DR2})/R_{\rm sis}$.

$M_{\rm DR2}$ of 1323 stars with $T_{\rm A}$ is plotted with respect to $M_{\rm sis}$ in Fig. 10. The fitted curve is found as

$$M_{\rm DR2} = (0.925 \pm 0.017)M_{\rm sis}^{0.698\pm0.037}.$$

For $T_{\rm G}$, if we use the same power (0.698), $M_{\rm DR2} = 0.884M_{\rm sis}^{0.698}$. These two curves are very similar to each other in Fig. 10. Also shown are the solar-like oscillating RGs in EBs. Their positions in Fig. 10 share the same area with the most of the 1323 stars, except the RG component with $M_{\rm sis}$ about 2.5 $\rm M_\odot$. For comparison, the 79 MS and SG stars are also plotted in Fig. 10. They take place above the solar-like oscillating RGs in EBs. The fitted curves for the 79 stars and 909 RGs are similar to each other. From Fig. 10 we see that there are two different relations between $M_{\rm DR2}$ and $M_{\rm sis}$. One is for 1323 RGS and another one is for the 909 RGs and the 79 (MS+SG) stars. When we compare the 909 stars with the 1323 stars, there is a remarkable difference between the $T_{\rm eff}$ of these two groups of stars. While the $T_{\rm eff}$s of the former group are mostly in the range 4600-5000 K, most of the latter group members is populated in 4500-4800 K. The difference between average $T_{\rm eff}$s of these two groups is 100 K. Similarly, there is a difference between

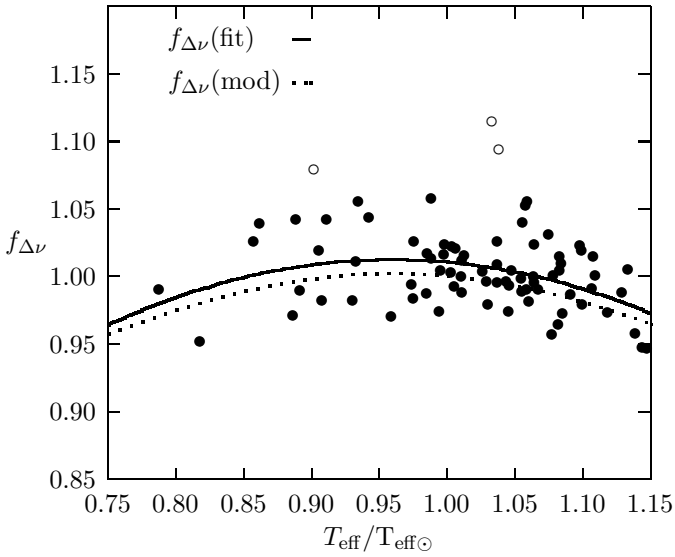

Figure 11. For the 79 stars, $f_{\Delta\nu}$ is plotted with respect to $T_{\rm eff}$ in solar units. The solid line is for the fitting curve obtained by excluding three stars (open circles) in the upper part of the figure, $(-1.096 \pm 0.299)(T_{\rm eff}/{\rm T}_{\rm eff\odot} - 0.96)^2 + 1.012 \pm 0.004$. The dotted line shows $f_{\Delta\nu{\rm mod}}$ derived from the interior models by Yıldız et al. (2016).

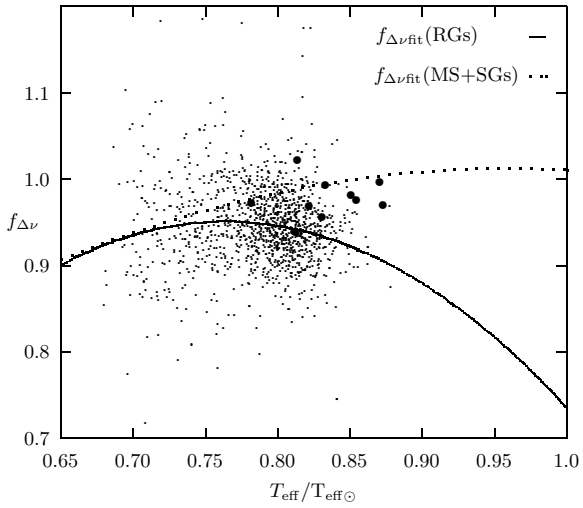

Figure 12. For the 1323 stars (dots), $f_{\Delta\nu}$ is plotted with respect to $T_{\rm eff}$ in solar units. The thick solid line is the fitting curve for these stars: $(-3.87 \pm 0.93)(T_{\rm eff}/{\rm T}_{\rm eff\odot} - 0.764 \pm 0.005)^2 + 0.951 \pm 0.002$. The dotted line shows the fitted curve for the 76 MS+SG stars (see Fig. 11). Also shown are the RGs in 10 EBs (the filled circles).

mean radii: $\delta R_{\rm DR2}$ is about 1.5 $R_\odot$. This implies that the 909 stars mostly occupy the lower part of the RG branch and the 1323 stars take place in the upper part of the branch.

The number of stars with a $T_{\rm eff}$ higher than 4850 K is 37 among the 1323 RGs and 179 among the 909 stars.

There are two different scaling relations for the RGs. The critical value for $\log g$ is about 2.6. The critical $T_{\rm eff}$ is about 4700-4800K. For $\log g$=2.6-3.5,

$$f_{\Delta\nu} = 0.0548 \log g + 0.800.$$

For $\log g$ =2.0-2.6,

$$f_{\Delta\nu} = -0.0220 \log g + 1.002.$$

The average effective temperature and $\log g$ of 1323 stars are 100 K and 0.20 less than $T_{\rm eff}$ and $\log g$ of the 909 stars, respectively. For the 909 stars,

$$M_{\rm DR2} = (1.012 \pm 0.040) M_{\rm sis}^{0.722 \pm 0.078}.$$

For the 89 stars,

$$M_{\rm DR2} = (1.092 \pm 0.024) M_{\rm sis}^{0.624 \pm 0.024}.$$

For the 10 EBs, if $n = 0.698$

$$M_{\rm DR2} = 0.929 M_{\rm sis}^{0.698}.$$

This is identical to the curve for 1323 RGs with $T_{\rm A}$. If we exclude the star with M=2.15, the fitting curve is exactly the same as that of 1323 RGs with $T_{\rm G}$: $M_{\rm DR2} = 0.884 M_{\rm sis}^{0.698}$.

4.6 $f_{\Delta\nu}$ and $f_{\nu_{\rm max}}$ from comparison of masses and radii

In principle, we can obtain expressions for $f_{\nu_{\rm max}}$ and $f_{\Delta\nu}$ from the ratio $M_{\rm DR2}/M_{\rm sis}$ and $R_{\rm DR2}/R_{\rm sis}$. Assuming $M_{\rm DR2}$ and $R_{\rm DR2}$ as exact values and using equations (9)-(10) in Yıldız et al. (2016), we obtain $f_{\nu_{\rm max}}$ and $f_{\Delta\nu}$ as $(R_{\rm DR2}/R_{\rm sis})^2/(M_{\rm DR2}/M_{\rm sis})$ and $\sqrt{(R_{\rm DR2}/R_{\rm sis})^3/(M_{\rm DR2}/M_{\rm sis})}$, respectively. For MS and SG stars, $f_{\Delta\nu}$ is a function of $T_{\rm eff}$ (or Γ_{1s}) as in Yıldız et al. (2016). $f_{\Delta\nu}$ of the 79 stars are plotted with respect to $T_{\rm eff}$ in Fig. 11. The three stars (KIC 8379927, KIC 9025370 and KIC 11772920) represented with the circle are taking in the upper part of Fig. 11. The fitting curve is obtained by neglecting these three stars as

$$f_{\Delta\nu} = (-1.096 \pm 0.299)({\rm T}_{\rm eff}/{\rm T}_{\rm eff\odot} - 0.96)^2 + 1.012 \pm 0.004. \quad (4)$$

Also shown is the $f_{\Delta\nu{\rm mod}}$ obtained from the interior models by Yıldız et al. (2016) due to a variation of Γ_{1s}. The difference between these two expressions for $f_{\Delta\nu}$ is almost constant and about 0.01. Such a small difference may be due to modelling of the outer regions or uncertainties in any of observed quantities such as $T_{\rm eff}$ and parallax ($\pi_{\rm DR2}$). For V and BC from Lejeune et al. (1998), $f_{\Delta\nu} = -1.286({\rm T}_{\rm eff}/{\rm T}_{\rm eff\odot} - 0.96)^2 + 1.017$.

Using this $f_{\Delta\nu}$, we find that $f_{\nu{\rm max}}$ does not depend on $T_{\rm eff}$ and is unity for 76 stars. This implies that the classical scaling relation for $\nu_{\rm max}$ is suitable for this group of stars.

One may use spectroscopically derived $\log g_{\rm S}$ in computation of $M_{\rm DR2}$ of the 79 stars, and try to obtain $f_{\nu_{\rm max}}$. However, accuracy of $\log g_{\rm S}$ does not permit to reach a definite relationship for $f_{\nu_{\rm max}}$. Since we employ the same $\log g_{\rm S}$ and $T_{\rm eff}$ in computation of $R_{\rm sis}$ and $R_{\rm DR2}$, one can not obtain an expression for $f_{\nu_{\rm max}}$ as for $f_{\Delta\nu}$.

Similarly, we can also derive an expression for $f_{\Delta\nu}$ of RGs. In Fig. 12, $f_{\Delta\nu}$ is plotted with respect to $T_{\rm eff}/T_{\rm eff\odot}$ for 1323 RG stars. We notice that the most of the stars have $f_{\Delta\nu}$ significantly less than 1. The fitting curve is obtained as

$$f_{\Delta\nu} = (-3.87 \pm 0.93)({\rm T}_{\rm eff}/{\rm T}_{\rm eff\odot} - 0.764 \pm 0.005)^2 + 0.951 \pm 0.002. \quad (5)$$

Its maximum value is 0.951. This implies that the corrections for $R_{\rm sis}$ and $M_{\rm sis}$ are about 10 and 20 per cent, respectively. Also shown in Fig. 12 is the fitting curve for the relatively hot 76 MS and SG stars. 10 solar-like oscillating RGs in EBs occur about the transition region from one curve to another one.

In Fig. 13, $M_{\rm DR2}$ is plotted with respect to the corrected $M_{\rm sis}$ ($M_{\rm cor}$) according to $f_{\Delta\nu}$ derived for 1323 RGs from Fig. 12. The relationship between $M_{\rm DR2}$ and $M_{\rm cor}$ is linear and the positions

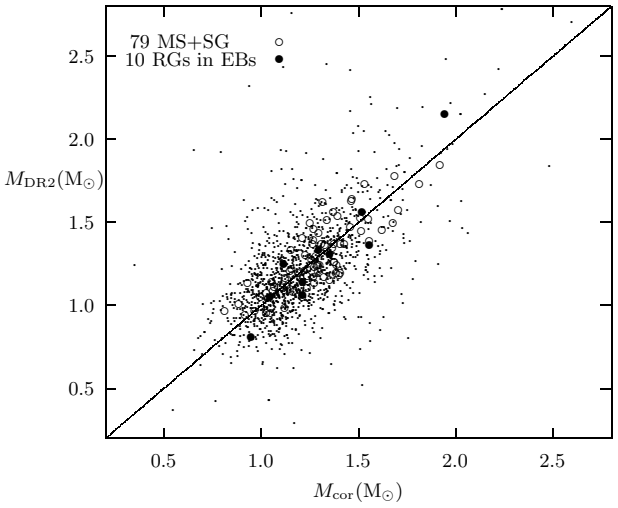

Figure 13. $M_{\rm DR2}$ of 1323 RG stars (dots) is plotted with respect to the corrected asteroseismic mass $M_{\rm cor}$ in solar units using $f_{\Delta\nu}$ derived from Fig. 13. $T_{\rm eff}$ of 1323 RGs are taken as $T_{\rm A}$. Also shown are the corrected radii of the 79 MS+SG stars (circle) and 10 RGs in EBs (filled circles).

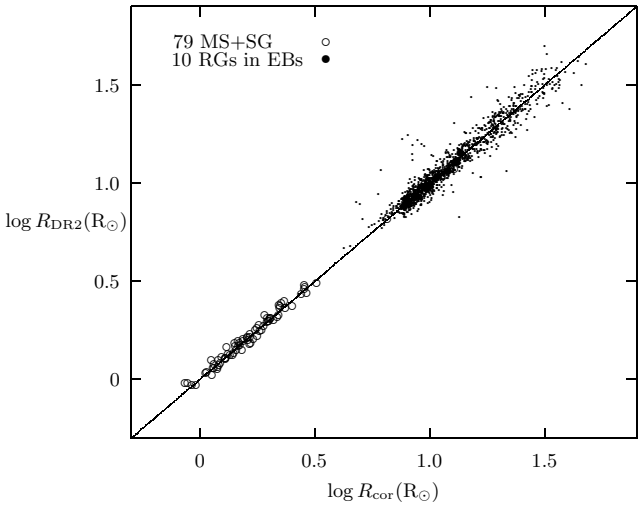

Figure 14. $R_{\rm DR2}$ of 1323 RG stars (dots) is plotted with respect to the corrected asteroseismic radius $R_{\rm cor}$ in solar units using $f_{\Delta\nu}$ derived from Fig. 13. $T_{\rm eff}$ of 1323 RGs are taken as $T_{\rm A}$. Also shown are the corrected radii of the 79 MS+SG stars (circle) and 10 RGs in EBs (filled circles).

of the most of the stars are close to the $M_{\rm DR2}$=$M_{\rm cor}$ line. Most of the stars have the mass in the 0.9-1.5 $\rm M_\odot$ range. However, there are also significant scattering. For 319 of 1323 RGs, the difference between $M_{\rm DR2}$ and $M_{\rm cor}$ is less than 5 per cent. There are some stars with mass $0.5 < M < 0.9\rm M_\odot$. The MS life time of these stars is greater than the age of the galaxy. Therefore, they can not be in the RG branch as long as these masses are their initial masses. On the other hand, at least for some of these stars both $M_{\rm cor}$ and $M_{\rm DR2}$ are small. This leads us to rely on the computed masses. Then, these stars might have experienced serious mass loss during their past evolution. For comparison, the 79 RGs and solar-like oscillating RGs in EBs are also plotted in Fig 13.

In Fig. 14, $\log R_{\rm DR2}$ is plotted with respect to $\log R_{\rm cor}$ according to $f_{\Delta\nu}$ derived for 1323 RGs from Fig. 12 and for the 76 stars from Fig. 11. $R_{\rm DR2}$ and $R_{\rm cor}$ are in very good agreement. $R_{\rm sis}$ of 10 RGs in EBs are computed using $f_{\Delta\nu}$ and $f_{\nu\rm max}$ derived from Figs. 6-7. $\log R_{\rm cor}/\rm R_\odot$ of these stars range from 0.89 to 1.14, and in very good agreement with the radii derived from light curve analysis of the EBs.

4.7 How $T_{\rm eff}$ is certain and solution with convenient $T_{\rm eff}$

If we compare $T_{\rm G}$ from *Gaia* Apsis and $T_{\rm A}$ from APOKASC2, we find significant differences between them. This leads us to test the effect of uncertainty of $T_{\rm eff}$ on the differences between asteroseismic ($d_{\rm sis}$, $R_{\rm sis}$ and $M_{\rm sis}$) and non-asteroseismic quantities ($d_{\rm DR2}$, $R_{\rm DR2}$ and $M_{\rm DR2}$). In this section, we try to make corrected $R_{\rm sis}$ and $R_{\rm DR2}$ equal by changing only $T_{\rm eff}$. We first clarify how $R_{\rm sis}$ and $R_{\rm DR2}$ are sensitive to change in $T_{\rm eff}$. For $R_{\rm sis}$, we find from the scaling relation that

$$\frac{\Delta R_{\rm sis}}{R_{\rm sis}} = \frac{1}{2}\frac{\Delta T_{\rm eff}}{T_{\rm eff}}. \quad (6)$$

For $R_{\rm DR2}$, the situation is a little more complicated. We first compute L from the absolute magnitude and BC. The change in $T_{\rm eff}$ influences BC and hence L. If we assume that the effect of change in $T_{\rm eff}$ on $R_{\rm DR2}$ over BC is negligibly small, then dependence of $R_{\rm DR2}$ is determined by $R_{\rm DR2} = (L/4\pi\sigma)^{1/2}/{T_{\rm eff}}^2$ (for the coolest stars this is not the case, see below). For a given value of L, we can show as

$$\frac{\Delta R_{\rm DR2}}{R_{\rm DR2}} = -2\frac{\Delta T_{\rm eff}}{T_{\rm eff}}. \quad (7)$$

While $R_{\rm sis}$ is proportional to ${T_{\rm eff}}^{1/2}$, $R_{\rm DR2}$ is inversely proportional to ${T_{\rm eff}}^2$. Since the $T_{\rm eff}$ dependencies of $R_{\rm sis}$ and $R_{\rm DR2}$ are completely different, we attempt to remove the difference between the asteroseismic and non-asteroseismic quantities, by changing only $T_{\rm eff}$.

The estimated $T_{\rm eff}$ (${T_{\rm eff}}'$) as a function of $R_{\rm sis}$ and $R_{\rm DR2}$ is found from equations (6) and (7) as

$${T_{\rm eff}}' = T_{\rm eff} + \Delta T_{\rm eff} = T_{\rm eff}(1 + x_T) \quad (8)$$

where

$$x_T = \frac{\Delta T_{\rm eff}}{T_{\rm eff}} = \frac{R_{\rm DR2} - R_{\rm sis}}{2R_{\rm DR2} + R_{\rm sis}/2}. \quad (9)$$

If $R_{\rm DR2}$ is less than $R_{\rm sis}$, then ${T_{\rm eff}}'$ is lower than $T_{\rm eff}$. In the other circumstance, ${T_{\rm eff}}'$ is higher than $T_{\rm eff}$.

BC is almost constant for about $5000 < T_{\rm eff} < 6000$ K. For $T_{\rm eff} < 4100$ K, however, BC is a very sensitive function of $T_{\rm eff}$. Therefore, we follow an iterative method to find the most appropriate ${T_{\rm eff}}'$ for a star for which $R_{\rm DR2} = R_{\rm sis}$. We first compute all the asteroseismic and non-asteroseismic quantities using the catalog value of $T_{\rm eff}$ and then find ${T_{\rm eff}}'$. We recompute all the quantities using the new effective temperature and repeat the procedure until effective temperature is fixed at a certain value.

For $T_{\rm eff} < 4100$ K, where $\partial BC/\partial T_{\rm eff}$ is not small, however, we find that the coefficient (-2) in the right side of equation (7) becomes $(-2-(\partial BC/\partial T_{\rm eff})T_{\rm eff}/5)$. Although the relation between BC and $T_{\rm eff}$ is not linear but we find the slope for $T_{\rm eff} < 4100$ K as 0.00464.

For the 1160 stars of 1323, value of ${T_{\rm eff}}'$ is between $T_{\rm A} - 200$ K and $T_{\rm A} + 200$ K. The number of stars for which either $|T'_{\rm eff} - T_{\rm A}| < 200$ or $|T'_{\rm eff} - T_{\rm G}| < 200$ K is 1217. For the 367 stars of 1323, value of ${T_{\rm eff}}'$ is between $T_{\rm G}$ and $T_{\rm A}$.

For the 1217 RGs ($|T'_{\rm eff} - T_{\rm A}| < 200$ or $|T'_{\rm eff} - T_{\rm G}| < 200$ K), a table is prepared for comparison of ${T_{\rm eff}}'$ with $T_{\rm A}$ and $T_{\rm G}$. The fundamental properties of these stars are perhaps among the most precise stellar data, provided that the accuracy of *Gaia* distances is good enough. This table will appear in the online version of the article. We recompute gravity ($\log g'_{\rm cor}$), mass ($M'_{\rm cor}$) and radius ($R'_{\rm cor}$ of these stars using ${T_{\rm eff}}'$ and the expression for $f_{\Delta\nu}$ (equation 4). A sample of the online table is given in Table 2. Release of

future accurate data of *Gaia* will make these quantities much more accurate than the present data.

5 PARALLAX OFFSET AND SCALING RELATIONS

The difference between asteroseismic and non-asteroseismic distance may arise either from difference between true ($\pi_{\rm true}$) and *Gaia* DR2 parallaxes or difference between true radius ($R_{\rm true}$) and $R_{\rm sis}$. If there is an offset, $\Delta\pi = \pi_{\rm DR2} - \pi_{\rm true}$ is a constant. $R_{\rm true}$ can be written as a function of $f_{\nu_{\rm max}}$ and $f_{\Delta\nu}$: $R_{\rm true} = f^2_{\Delta\nu}/f_{\nu_{\rm max}} R_{\rm sis}$. If $R_{\rm sis}$ is perfect then $f_{\Delta\nu} = f_{\nu_{\rm max}} = 1$, defect is pertaining to the *Gaia* DR2 data and one can obtain $\Delta\pi$. If $\pi_{\rm DR2}$ is perfect, then $\Delta\pi = 0$ and we can at least find $f^2_{\Delta\nu}/f_{\nu_{\rm max}}$ from the relation between $R_{\rm true}$ and $R_{\rm sis}$ (see below). However, we can do something better than these two options, if one may obtain a relationship between $f^2_{\Delta\nu}$, $f_{\nu_{\rm max}}$ and $\Delta\pi$.

Radius and distance of a star are interrelated over its luminosity. We assume $T_{\rm eff}$, V and BC are given. If we determine radius, from asteroseismic scaling relations, for example, then one can find distance from the comparison of flux at the surface of the star and flux we receive. If we know radius, we can determine distance or vice versa. If the difference between "true" and estimated radii is, for example, 2 per cent, then the difference between true and estimated distances is 2 per cent too. This implies that $R_{\rm true}/R_{\rm est} = d_{\rm true}/d_{\rm est}$.

This is the case for both sets of the quantities based on *Gaia* DR2 parallax and asteroseismic scaling relations.

$$R_{\rm true} = R_{\rm DR2} d_{\rm true}/d_{\rm DR2} = R_{\rm DR2}/(1 + \Delta\pi d_{\rm DR2}).$$

Using the relation between $R_{\rm sis}$ and $R_{\rm true}$,

$$R_{\rm true} = f^2_{\Delta\nu}/f_{\nu_{\rm max}} R_{\rm sis} = R_{\rm DR2}/(1 + \Delta\pi d_{\rm DR2}).$$

Then,

$$f_{\nu_{\rm max}} = R_{\rm sis}/R_{\rm DR2}(1 + \Delta\pi d_{\rm DR2}) f^2_{\Delta\nu}. \qquad (10)$$

For MS stars we know $f_{\Delta\nu}$ from the models. Then, we have a relationship between $f_{\nu_{\rm max}}$ and $\Delta\pi$ from equation (10).

Similarly, we can find another relation between $f_{\Delta\nu}$, $f_{\nu_{\rm max}}$ and $\Delta\pi$ from the ratio of $M_{\rm sis}$ and $M_{\rm DR2}$:

$$f_{\nu_{\rm max}} = (M_{\rm sis}/M_{\rm DR2})^{0.5}(1 + \Delta\pi d_{\rm DR2}) f^2_{\Delta\nu}.$$

Hence,

$$M_{\rm sis}/M_{\rm DR2} = (R_{\rm sis}/R_{\rm DR2})^{0.5}$$

or

$$\delta M/M = 2\delta R/R.$$

Since we use the same gravity ($g_{\rm sis}$) for the both methods, $\delta g/g = \delta M/M - 2\delta R/R = 0$. This is the underlying reason behind the result for $\delta M/M = 2\delta R/R$.

5.1 Parallax offset for the MS and SG stars

Assume the difference between two $f_{\Delta\nu}$ is due to offset and $f_{\nu_{\rm max}}$=1. In order to equalize the asteroseismic and non-asteroseismic radii to each other, we obtain $\Delta\pi$ for 76 stars as -0.125 mas. $\Delta\pi$ of -0.125 mas gives us the mean value of

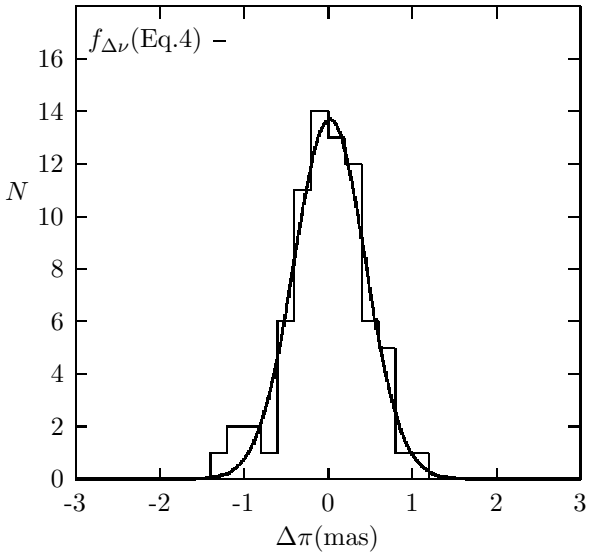

Figure 15. Histogram for the 75 stars with $f_{\Delta\nu}$ given in Fig. 11.

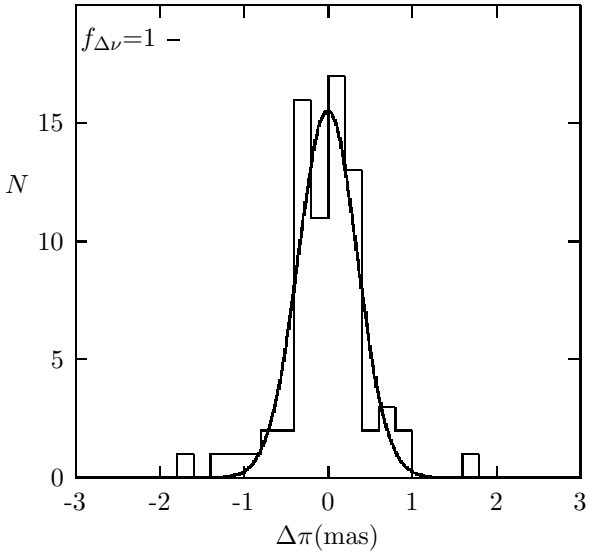

Figure 16. Histogram for the 75 stars with $f_{\Delta\nu}$ =1.

$R_{\rm sis}/R_{\rm DR2}$ as 1. However, with this amount of offset, $f_{\nu_{\rm max}}$ shows $T_{\rm eff}$ dependence.

If the offset is zero and $f_{\Delta\nu}$ is the same as obtained in Yıldız et al. (2016), then $f_{\nu_{\rm max}} \simeq 0.98$. However, $f_{\nu_{\rm max}}$ has $T_{\rm eff}$ dependence if there is an offset. If $\Delta\pi$ is the same as obtained by Stassun & Torres (2018) for eclipsing binaries, -0.082 mas, for example, we obtain $f_{\nu_{\rm max}}$ ($\nu_{\rm max\odot}$=3050) as $f_{\nu_{\rm max}} = 0.789(T_{\rm eff}/{\rm T_{eff\odot}})^2 - 1.622(T_{\rm eff}/{\rm T_{eff\odot}}) + 1.823$. For this $\Delta\pi$ and $\nu_{\rm max\odot}$=3050, $f_{\nu_{\rm max}}(1)$=0.99. If $\Delta\pi$ is taken as 0.173 mas, $f_{\nu_{\rm max}}(1)$=1:

$$f_{\nu_{\rm max}} = 1.604(T_{\rm eff}/{\rm T_{eff\odot}})^2 - 3.307(T_{\rm eff}/{\rm T_{eff\odot}}) + 2.703.$$

For $\nu_{\rm max\odot}$=3020, $f_{\nu_{\rm max}} = 0.796(T_{\rm eff}/{\rm T_{eff\odot}})^2 - 1.636(T_{\rm eff}/{\rm T_{eff\odot}}) + 1.840$. For the Sun, $f_{\nu_{\rm max}}$ =1.

If we use $f_{\Delta\nu}$ derived for 76 stars in section 4.6, we find that $|\Delta\pi|$ is less than 1.4 mas for 75 of the stars. For only HD 203608, it is about 7 mas. The offset for the 75 stars is very small, 0.0039

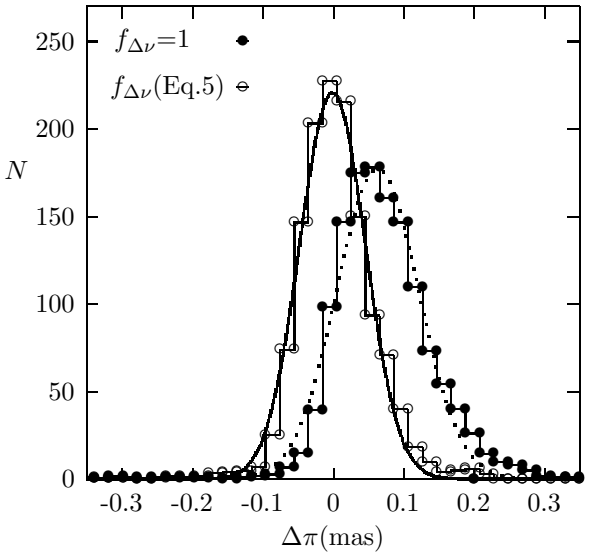

Figure 17. Histogram for the 1323 RGs with $f_{\Delta\nu} = 1$ (filled circles) and $f_{\Delta\nu}$ given (circles) in equation (5).

mas. This amount of offset gives us $f_{\nu_{\rm max}}$ =1. This implies that the classical scaling relation for $\nu_{\rm max}$ is valid for this group of stars, mostly consists of MS and SG stars. The histogram of the 75 stars is plotted in Fig. 15. The distribution is very likely a gaussian curve.

If $f_{\Delta\nu} = f_{\nu_{\rm max}} = 1$, $\Delta\pi$=-0.0761 mas for the 75 stars. The histogram of the 75 stars is plotted in Fig. 16. The distribution is not well represented by a gaussian curve. Using this $\Delta\pi$ we recompute $f_{\Delta\nu}$ and find that

$$f_{\Delta\nu} = -1.584(T_{\rm eff}/{\rm T}_{\rm eff\odot})^2 + 3.084(T_{\rm eff}/{\rm T}_{\rm eff\odot}) - 0.4890.$$

In this case, $f_{\nu_{\rm max}}$ is unity.

If $\Delta\pi$=-0.050 mas, about the typical value in the literature,

$$f_{\Delta\nu} = -1.291(T_{\rm eff}/{\rm T}_{\rm eff\odot})^2 + 2.507(T_{\rm eff}/{\rm T}_{\rm eff\odot}) - 0.208.$$

Using this $\Delta\pi$ and $f_{\Delta\nu}$, we find that $f_{\nu_{\rm max}}$ is almost constant and its mean value is about unity.

5.2 Parallax offset for RG stars

We have already derived $f_{\Delta\nu}$ for 1323 RGs (see section 4.6) assuming no offset. If we take $f_{\Delta\nu} = f_{\nu_{\rm max}} = 1$, then we can find value of $\Delta\pi$. For this case, $\Delta\pi$ is about 0.0696 mas. Histogram of these stars is plotted in Fig. 17. Distribution of stars (filled circles) is not well represented by a gaussian curve (dotted line).

If $f_{\Delta\nu}$ given in equation (5) is employed, we find that $\Delta\pi$ is equal to 0.00230 mas. Histogram of these stars are also plotted in Fig. 17. The distribution for this case (circles) is more likely gaussian than that of the data with $f_{\Delta\nu}$=1.

If we take $\Delta\pi$ as -0.082 mas, for example, the mean value of $f_{\Delta\nu}$ is about 0.88, significantly less than 1. This implies that much more correction is required for the negative values of $\Delta\pi$ for the RGs.

For 75 stars, $\Delta\pi$ is less than zero, while it is positive for 1323 RGs, 0.0696 mas. This implies that improvement in asteroseismic scaling relations is an obligation rather than choice for the agreement

6 CONCLUSIONS

Combining all photometric, spectral, astrometric and asteroseismic data, we find distance, radius and even mass of about 1800 stars from two different methods and compare these findings in order to assess *Gaia* parallaxes and to improve the asteroseismic scaling relations for stellar mass and radius. In this regard, *Gaia*, *Kepler* and *TESS* space projects open a new era in our understanding of stellar evolution theory.

We first compare the first two data releases of *Gaia*. The DR2 parallaxes are much more accurate than the DR1 parallaxes. The 5 per cent systematic difference between $d_{\rm sis}$ and $d_{\rm DR1}$ (Yıldız et al. 2017) reduces to 1.1 per cent for $d_{\rm DR2}$ for the 79 (MS + SG + 2RGs) stars. From the comparison of $R_{\rm sis}$ and $R_{\rm DR2}$, we obtain that $R_{\rm DR2} = 1.052R_{\rm sis}^{0.935}$. Since there are only 2 RGs in this sample, we extend our study to the RGs in the APOKASC2 catalog. There are two samples of RGs we analyze. Luminosities of the stars are computed from the V magnitude for one group (909 RGs) and from the *Gaia* G magnitude for the other group (1323 RGs). About 493 RGs are common in both groups. From the comparison of $R_{\rm sis}$ and $R_{\rm DR2}$, we obtain relationships very similar to the relationship for the 79 stars. These relationships leads us to show how to improve the conventional scaling relations. Similar relationships are valid also for the RGs in EBs. We also find relationship between $M_{\rm sis}$ and $M_{\rm DR2}$. From the ratio $\sqrt{(R_{\rm DR2}/R_{\rm sis})^3/(M_{\rm DR2}/M_{\rm sis})}$, we find the expression for $f_{\Delta\nu}$. This expression for the 76 stars is almost identical to the one we have obtained from interior models for MS stars. For RGs with $T_{\rm eff}$ less than about 4800 K, there is another relationship in particular for 1323 RGs. Using these expressions for $f_{\Delta\nu}$, we can improve $M_{\rm sis}$ and $R_{\rm sis}$. Such a correction for $R_{\rm sis}$ and $M_{\rm sis}$ of RGs in EBs makes them in agreement with radius and mass derived from orbital analysis.

Finally, improvement for M and R can be done over $T_{\rm eff}$, because the dependencies of asteroseismic ($d_{\rm sis}$, $R_{\rm sis}$ and $M_{\rm sis}$) and non- asteroseismic quantities ($d_{\rm DR2}$, $R_{\rm DR2}$ and $M_{\rm DR2}$) on $T_{\rm eff}$ are completely different. While $R_{\rm sis}$, for example, is proportional to $T_{\rm eff}^{1/2}$, $R_{\rm DR2} \propto T_{\rm eff}^{-2}$ for RGs with $T_{\rm eff} > 4100$ K. Therefore, slight modifications in $T_{\rm eff}$ remove all the differences between asteroseismic and non-asteroseismic quantities for most of the stars. For the RGs with $T_{\rm eff} < 4100$ K, we also take into account derivative of BC with respect to $T_{\rm eff}$.

ACKNOWLEDGEMENTS

Daniel Huber, M. Salaris and Antonio Frasca are acknowledged for their discussions. We would like to thank Dr. Frederick A. Magill for his professional checking language of the paper.

Table 2. Basic properties of the 1217 RGs for which we compute the most appropriate effective temperature $T'_{\rm eff}$ from equation (8). Columns are organized as star name, $T'_{\rm eff}$, $\Delta T'_{\rm eff}$, the corrected mass and its uncertainty, the corrected radius and its uncertainty, metallicity and its uncertainty, the corrected gravity and its uncertainty. $\Delta T'_{\rm eff}$ is taken as $|T'_{\rm eff} - (T_{\rm A} + T_{\rm G})/2|$. $\Delta M'_{\rm cor}$, $\Delta R'_{\rm cor}$ and $\Delta \log g'_{\rm cor}$ are computed from the scaling relations with a quadratic approach.

KIC	$T'_{\rm eff}$ (K)	$\Delta T'_{\rm eff}$ (K)	$T_{\rm A}$ (K)	$T_{\rm G}$ (K)	$M'_{\rm cor}$ ($M_\odot$)	$\Delta M'_{\rm cor}$ ($M_\odot$)	$R'_{\rm cor}$ ($R_\odot$)	$\Delta R'_{\rm cor}$ ($R_\odot$)	[Fe/H]	Δ[Fe/H]	$\log g'_{\rm cor}$ (cgs)	$\Delta \log g'_{\rm cor}$ (cgs)
1719297	4241	4	4232	4241	1.10	0.03	23.33	0.44	-0.02	0.02	1.744	0.009
2300503	4363	53	4404	4428	1.17	0.02	17.29	0.17	-0.13	0.03	2.031	0.009
2301349	4496	119	4603	4627	1.25	0.04	8.05	0.15	0.39	0.02	2.722	0.019
2422073	4473	16	4489	4492	1.11	0.01	12.05	0.04	0.09	0.03	2.320	0.003
2140446	4492	62	4549	4561	1.22	0.02	8.58	0.09	0.30	0.02	2.657	0.010
1872469	4603	45	4657	4639	1.18	0.01	8.45	0.06	0.14	0.03	2.657	0.007
1725552	4248	17	4325	4135	1.39	0.02	25.02	0.25	0.10	0.02	1.784	0.007
1433730	4560	118	4727	4630	1.59	0.05	11.68	0.22	-0.03	0.03	2.504	0.018
1725732	3992	96	4077	4100	0.82	0.08	30.66	1.99	0.07	0.02	1.381	0.023
2017541	4143	43	4208	4166	1.15	0.04	20.90	0.44	0.14	0.02	1.858	0.008
1572780	4658	113	4784	4759	0.80	0.02	12.19	0.22	-0.51	0.04	2.171	0.017
1432587	4288	91	4288	4470	0.80	0.03	22.57	0.48	-0.20	0.03	1.634	0.019
1433593	4747	27	4778	4771	1.45	0.01	8.47	0.04	0.16	0.03	2.744	0.004
1163114	4145	172	4285	4350	1.35	0.07	18.41	0.55	0.30	0.02	2.038	0.029
1871927	4604	57	4650	4674	1.14	0.02	7.71	0.07	0.20	0.03	2.722	0.009
1163359	4727	113	4571	4655	1.43	0.04	15.01	0.26	-0.34	0.03	2.242	0.017
1871314	4567	66	4552	4450	1.30	0.02	8.73	0.09	0.35	0.02	2.669	0.010
2305590	4546	129	4603	4746	1.00	0.04	8.40	0.17	-0.30	0.03	2.591	0.020
2014684	4286	5	4303	4280	0.92	0.03	23.29	0.47	-0.26	0.03	1.665	0.006

REFERENCES

Baglin A., Michel E., Auvergne M., COROT Team, 2006, in Fridlund M., Baglin A., Lochard J., Conroy L., eds, ESA Special Publication Vol. 1306, ESA Special Publication. p. 33

Borucki W. J., Koch D., Basri G., et al. 2010, Science, 327, 977

Chaplin W. J., Miglio A., 2013, ARA&A, 51, 353

Choi, J., Dotter, A., Conroy, C., Cantiello, M., Paxton, B., Johnson, B. D., 2016, ApJ, 823, 102

Davies G. R., Lund M. N., Miglio A., 2017, A&A, 598, L4

De Ridder J., Molenberghs G., Eyer L., Aerts C., 2016, A&A, 595, L3

Gaia Collaboration, Brown A. G. A., Vallenari A., et al. 2016, A&A, 595, A2

Gaia Collaboration, Brown A. G. A., et al., 2018, A&A, 616, A1

Gaulme P., McKeever J., Jackiewicz J., et al., 2016, ApJ, 832, 121

Huber D., Zinn J., Bojsen-Hansen M., et al., 2017, ApJ, 844, 102

Kallinger T., Beck P. G., Stello D., Garcia R. A., 2018, A&A, 616, A104

Kjeldsen H., Bedding T. R., 1995, A&A, 293, 87

Lejeune T., Cuisinier F., Buser, R., 1998, A&AS, 130, 65

Pinsonneault M. H., Elsworth Y. P. Tayar J., 2018, ApJS, 239, 32

Sahlholdt C. L., Silva Aguirre V., 2018, MNRA, 476, 1931

Stassun K. G., Torres G., 2018, ApJ, 862, 61

Sullivan P. W. et al., 2015, ApJ, 809, 77

Yıldız M., Çelik Orhan Z., Kayhan C., 2016, MNRAS, 462, 1577

Yıldız M., Çelik Orhan Z., Örtel S., Roth M., 2017, MNRAS, 470, 25

Yıldız M., Çelik Orhan Z., Kayhan C., 2019, MNRAS, 489, 1753

Zinn J. C., Pinsonneault M. H., Huber D., Stello D., 2019, ApJ, 878, 136